Chinese Chemical Letters 36 (2025) 109744

Contents lists available at ScienceDirect

Chinese Chemical Letters

journal homepage: www.elsevier.com/locate/cclet

A novel supramolecular assembly based on *nor-seco*-cucurbit[10]uril for spermine sensing and artificial light-harvesting

Ran Cen, Yan-Yan Tang, Li-Xia Chen, Zhu Tao, Xin Xiao*

National Key Laboratory of Green Pesticide, State Key Laboratory of Green Pesticide and Agricultural Bioengineering, Ministry of Education, Key Laboratory of Macrocyclic and Supramolecular Chemistry of Guizhou Province, Guizhou University, Guiyang 550025, China

ARTICLE INFO

Article history:
Received 25 December 2023
Revised 28 February 2024
Accepted 7 March 2024
Available online 8 March 2024

Keywords:
Nor-seco-cucurbit[10]uril
Perylene diimide derivative
Spermine
Light-harvesting

ABSTRACT

A supramolecular assembly composed of perylene diimide derivative (PDI-nm) and *nor-seco*-cucurbit[10]uril (*ns*-Q[10]) was designed. The excellent host-guest interaction between PDI-nm and *ns*-Q[10] prevented the aggregation-caused quenching (ACQ) effect of PDI-nm, resulting in a luminescent assembly. The addition of spermine to the PDI-nm/*ns*-Q[10] assembly restored the ACQ of PDI-nm due to the competitive binding of spermine to *ns*-Q[10], which released PDI-nm. The assembly based on this principle showed ultra-high sensitivity for the detection of spermine with a detection limit as low as 7.84×10^{-7} mol/L in aqueous solution and 3.69×10^{-7} mol/L in plasma solution. Moreover, an artificial light-harvesting system based on this assembly was proposed, benefiting from its good luminescent performance. Nile red (NiR) functioned as an acceptor loaded into assembly, and a highly efficient energy transfer process occurred from PDI-nm/*ns*-Q[10] to NiR, with an efficiency up to 87%.

Spermine is a bioactive polyamine that is abundant in living cells [1,2]. However, the concentration of spermine is elevated in patients with lung cancer, prostate cancer and liver tumor [3]. In addition, excessive intake of spermine can lead to respiratory distress, headache, hypertension and vomiting [4]. Therefore, the detection of biogenic amines involves public health problems [5,6], and their determination deserves attention. Conventional methods for determining spermine include HPLC, thin layer chromatography, capillary electrophoresis and so on. In the present work, our aim was to construct an indicator displacement assay (IDA) for the fluorescence sensing of spermine. various host–guest interactions have been exploited to design supramolecular-based molecular sensors, known as indicator displacement assays (IDAs) [7–9]. IDAs are based on the competitive binding of the analyte and a fluorescent indicator to a supramolecular host [10]. Therefore, simple, sensitive and preferably *in vivo* probes for trace spermine are greatly desirable for not only biomedical research but also environmental monitoring.

Simulated natural light-harvesting systems have good potential applications in the fields of biological imaging and optoelectronic devices [11–13]. Inspired by nature, there are two key conditions to realize efficacious energy transfer from a donor to an acceptor through the Föster resonance energy transfer (FRET) process [14,15]. Firstly, the donor should not only be densely packed, but also avoid self-quenching of intramolecular fluorescence caused by the aggregation-caused quenching (ACQ) effect. Secondly, the ratio of the donor to acceptor should be relatively high to ensure that multiple donors correspond to one acceptor. In addition, natural light-harvesting systems are constructed through the non-covalent interactions between chlorophyll and protein. However, supramolecular light-harvesting systems are constructed by non-covalent interactions and without multiple syntheses [16,17].

Macrocyclic hosts with double cavities are excellent materials for constructing supramolecular assembly. In the family of cucurbit[*n*]urils ($n = 5$–8, 10, 13–15) [18–24], *nor-seco*-cucurbit[10]uril (*ns*-Q[10]), as a special double cavity compound with rigid structure, which was synthesized and discovered by Isaacs in 2006 [25]. After almost twenty years of research and exploration, *ns*-Q[10] has been applied to molecular recognition [26–30], supramolecular hydrogel [31], supramolecular polymers [32] and so on. In the study of supramolecular polymers based on *ns*-Q[10], Isaacs designed and functionalized poly(*N*-hydroxyethylacrylamide) assembly with viologen, followed by addition of *ns*-Q[10] through specific and targeted bonding to form a ternary host-guest polymer [33]. Zhang fabricated *ns*-Q[10] based supramolecular assembly *via* self-sorting [34]. Recently, Yang and Li constructed a linear supramolecular dynamic rotaxane assembly by *ns*-Q[10], Q[7] and long liner derivatives of 4,4′-bipyridinium [35]. The aforementioned results jointly make clear that *ns*-Q[10]-based ternary complexation is a versatile platform for constructing various supramolecular polymers.

* Corresponding author.
E-mail addresses: gyhxxiaoxin@163.com, xxiao@gzu.edu.cn (X. Xiao).

https://doi.org/10.1016/j.cclet.2024.109744
1001-8417/

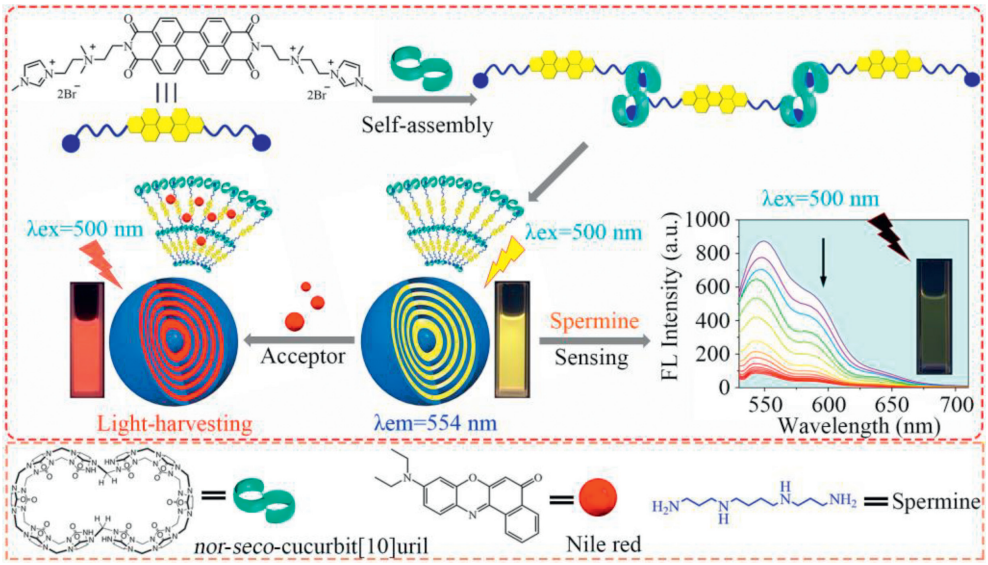

Scheme 1. Schematic illustration of PDI-nm/*ns*-Q[10] assembly for the sensing of spermine and the construction of light-harvesting system.

Herein, we designed and constructed an aqueous PDI-nm/*ns*-Q[10] assembly, which was based on the non-covalent host-guest interactions of a macrocyclic host *nor-seco*-cucurbit[10]uril (*ns*-Q[10]), a perylene bis(diimide) derivative (PDI-nm) as guest. There are two main purposes of introducing *ns*-Q[10] as the macrocyclic host: (1) the PDI-based chromophores are generally hydrophobic and show strong aggregation-caused quenching (ACQ) effect driven by $\pi-\pi$ stacking in aqueous solution [36,37], so the chromophore needs to be sufficiently separated to minimize self-quenching. By assembling *ns*-Q[10] and PDI-nm, PDI-nm can be prevented from self-aggregating and a PDI-nm/*ns*-Q[10] assembly with high emission can be obtained. (2) the *ns*-Q[10] host has an inherent double cavity structure, which can form host-guest inclusion complexes PDI-nm/*ns*-Q[10] with methyl imidazole groups of PDI-based derivatives, and further assemble to form microspheres. Therefore, according to the above research, we have constructed a multifunctional supramolecular assembly based on *ns*-Q[10] (Scheme 1). On the one hand, PDI-nm/*ns*-Q[10] assembly was applied to the sensing of spermine in aqueous solution and in plasma solution based on the principe of IDAs. The detection limit of assembly PDI-nm/*ns*-Q[10] towards the spermine could reach about 7.84×10^{-7} mol/L and 3.69×10^{-7} mol/L, respectively. On the other hand, an artificial light-harvesting system was constructed by using this assembly as donor and Nile red (NiR) as acceptor in aqueous solution. The PDI-nm/*ns*-Q[10]-NiR system showed a high energy transfer efficiency. This was of great significance for better understanding and simulating the natural light-harvesting antenna systems.

A comprehensive account of the synthesis, characterization, and analysis of the perylene diimide derivative, PDI-nm, was available in Scheme S1, Figs. S1 and S2 (Supporting information). Initially, supramolecular interaction of *ns*-Q[10] and PDI-nm was investigated by UV–vis and fluorescence spectra (Figs. 1a and b), the PDI-nm (1×10^{-5} mol/L) exhibited two adsorption peaks at 500 nm and 537 nm in aqueous solution. With the gradual increase of *ns*-Q[10], the Abs_{500} gradually decreases, and Abs_{537} gradually increases, accompanied by an equal absorption point appears at 514 nm, which was attributed to the shielding interaction of *ns*-Q[10]. Meanwhile, fluorescence intensity increased sharply, which was attributed to *ns*-Q[10] can form a host-guest complex with PDI-nm, inhibiting the $\pi-\pi$ stacking aggregation of PDI-nm and thus boosting the fluorescence intensity remarkably. The molar titration plots confirmed that the binding stoichiometry of the host *ns*-Q[10] with

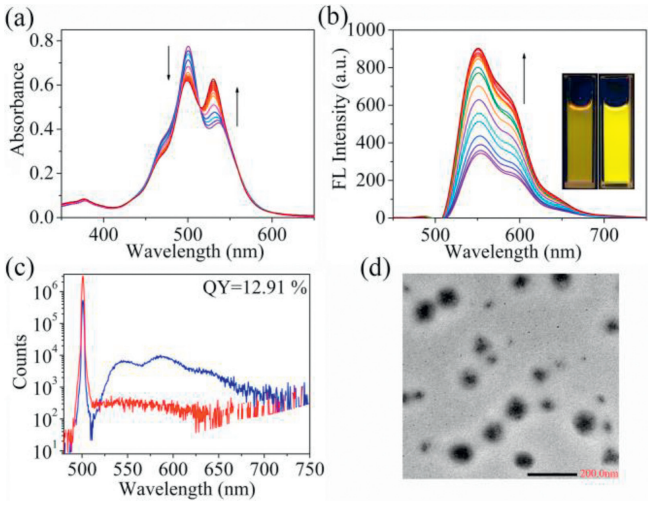

Fig. 1. (a) UV−vis absorption and (b) fluorescence spectral changes of PDI-nm (1×10^{-5} mol/L) after adding 2.0 equiv. of *ns*-Q[10] in aqueous solution, inset: images of PDI-nm (left) and PDI-nm/*ns*-Q[10] (right) under 365 nm light. (c) Fluorescence quantum yield of PDI-nm/*ns*-Q[10]. (d) TEM images of PDI-nm/*ns*-Q[10] assembly.

the guest PDI-nm was 1:1 in aqueous solution (Figs. S3 and S4 in Supporting information). The Job's plots was further demonstrated to form a 1:1 host-guest inclusion complex through UV–Vis and fluorescence spectra (Fig. S5 in Supporting information). Moreover, as shown in Fig. S6 (Supporting information), the HR-MS of PDI-nm/*ns*-Q[10] also showed the 1:1 stochiometric ratio. After complexation with *ns*-Q[10] in aqueous solution at a molar ratio of 1:1 (PDI-nm/*ns*-Q[10]), the maximum emission wavelength of PDI-nm/*ns*-Q[10] was at 500 nm with a strong emission band, and the fluorescence quantum yield was 12.91% (Fig. 1c), and the maximum emission wavelength exhibited the lifetime was 5.09 ns (Fig. S7 in Supporting information).

Further analysis of the modes of action using ^{1}H NMR spectroscopic technique, Fig. S8 (Supporting information) showed the corresponding ^{1}H NMR titration spectra. When 1.0 equiv. of *ns*-Q[10] was added, the signals corresponding to the 1-methylimidazole cation ($H_{e,i,j,h}$) protons of the guest PDI-nm shifted upfiled, while the remainder protons (H_{a-d}, H_{f-g} and H_{k-l}) of the PDI-nm shifted

downfield. This clearly indicated that 1-methylimidazole cation moieties were buried inside the hydrophobic cavity of the *ns*-Q[10], while the remainder moieties of the guest PDI-nm reside outside of the *ns*-Q[10] portals. Meanwhile, the signals in the aromatic region were weak and noisy, which indicated that the PDI-nm aromatic rings were in the aggregated state. In contrast, the ^{1}H NMR spectrum for the PDI-nm/*ns*-Q[10] assembly became clearer and the peaks were separated from each other, which indicated that the *ns*-Q[10] inhibited the close π-π stacking of the PDI-nm chromophores in the assembly [38–40].

Dynamic light scattering (DLS), Tyndall effect, transmission electron microscope (TEM) and fluorescence microscopy images were used to investigated the induced aggregation behavior of PDI-nm/*ns*-Q[10] assembly. DLS (Fig. S9 in Supporting information) revealed that the average hydrodynamic diameter of the nanospheres was 229.9 nm upon equimolar mixing of *ns*-Q[10] and PDI-nm, indicating the formation of highly polymerised supramolecular assembly. Then, the simple mixing of *ns*-Q[10] and PDI-nm exhibited obvious Tyndall effect in aqueous solution, which also indicated that a large supramolecular assembly was formed. But under the same conditions, only PDI-nm did not exhibit Tyndall effect, which indicated that PDI-nm did not form large self-aggregates. The high affinity between *ns*-Q[10] and PDI-nm resulted in the formation of supramolecular nanospheres with a ball structure, as shown by transmission electron microscopy (TEM, Fig. 1d). The PDI-nm/*ns*-Q[10] solution was dropped onto a glass slide to prepare a thin film. Under fluorescence microscope, the film emits intense red light, while the thin film of PDI-nm was scarcely emissive (Fig. S10 in Supporting information).

To demonstrate the sensing of PDI-nm/*ns*-Q[10], we investigated the response of PDI-nm/*ns*-Q[10] to spermine in aqueous solution. Spermine can preferably bind to *ns*-Q[10] due to the existence of multiple positive charges and long alkyl chains [41,42]. The experimental results suggested that spermine exhibits a binding affinity with *ns*-Q[10], one molecular. The binding constant of spermine and *ns*-Q[10] was 5.411×10^5 L/mol, significantly higher than that of PDI-nm and *ns*-Q[10] (Figs. S11-S13 in Supporting information). This leads to the dissociation of the supra-amphiphiles and concurrent quenching of the fluorescence. The free Perylene diimide (PDI) derivative, PDI-nm, tended to form non-fluorescent π-π stacks in aqueous. Therefore, the fluorescence of PDI-nm/*ns*-Q[10] was quenched. As shown in Figs. 2a and c, after spermine was added, the absorption intensity of PDI-nm/*ns*-Q[10] solution gradually weakened, and the color changed from pink to transparent under natural light (Fig. S14 in Supporting information). A notable thing was that a new absorption band was observed in the wavelength region around 577−620 nm upon stepwise addition of spermine, accompanied by the appearance of one isosbestic points and bathochromic shift. The phenomena confirmed the intermolecular charge transfer interaction arising from the $\pi-\pi$ stacking of the PDI-nm chromophores on accounts of the competitive complexation of spermine with *ns*-Q[10] [43]. Subsequently, the fluorescence changes of PDI-nm/*ns*-Q[10] during the increase of spermine content were tested. With the addition of spermine, the fluorescence emission intensity around 554 nm gradually decreased (Fig. 2b). The fluorescence intensity at 554 nm was almost quenched when the concentration of spermine reached 4×10^{-5} mol/L (illustration of Fig. 2b). As shown by Fig. S15 (Supporting information), the fluorescence intensity of PDI-nm/*ns*-Q[10] no longer decreased when the concentration of spermine reached 4×10^{-5} mol/L, and 4×10^{-5} mol/L spermine was selected in the following experiment. There was a good linear relationship between the decrease of fluorescence intensity and the increase of spermine concentration (3.6×10^{-5} – 6.3×10^{-5} mol/L, Fig. 2d). According to the formula LOD = $3\sigma/k$ (σ is the standard deviation of 10 blank samples, k is the slope of fluorescence intensity (I_{554nm})

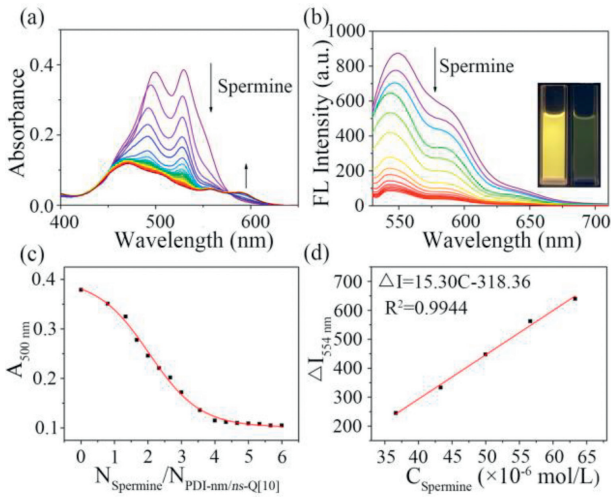

Fig. 2. (a) UV–vis adsorption and (b) fluorescence spectra of PDI-nm/*ns*-Q[10] (1×10^{-5} mol/L) with the addition of different concentrations of spermine ($0–4 \times 10^{-5}$ mol/L). Inset: photographs of PDI-nm/*ns*-Q[10] (left), and PDI-nm/*ns*-Q[10]-spermine under UV light (right). (c) The change of absorbance at the absorption wavelength of 500 nm. (d) Linear relationship between PDI-nm/*ns*-Q[10] fluorescence intensity and spermine concentration.

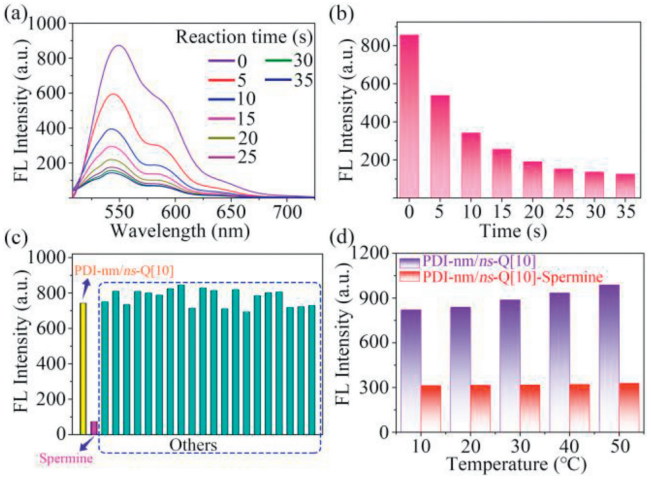

Fig. 3. (a) Fluorescence spectra of PDI-nm/*ns*-Q[10] (1×10^{-5} mol/L) solution in the presence of spermine (4×10^{-5} mol/L) at different times intervals. (b) The fluorescence intensity of 554 nm after adding spermine for different time. (c) Fluorescence changes of PDI-nm/*ns*-Q[10] (1×10^{-5} mol/L) after treated by spermine and others (L-Trp, L-Met, L-Thr, L-Val, L-Lys, L-Leu, L-Iso, L-Phe, TY, TMA, DA, Cu^{2+}, Mn^{2+}, Fe^{3+}, CO_3^{2-}, Br^-, SO_3^{2-}, NO_3^-, HPO_4^{2-}, F^- (4×10^{-5} mol/L, respectively)). (d) Thermostability of PDI-nm/*ns*-Q[10].

against spermine concentration) recommended by IUPAC, the detection limit (LOD) was as low as 7.84×10^{-7} mol/L. The binding kinetics of PDI-nm/*ns*-Q[10] and spermine were investigated, which reached the plateau within 35 s (Figs. 3a and b). Binding kinetics were faster than covalent reaction rate. When PDI-nm/*ns*-Q[10] reached the plateau, the quenching effect kept stable, and this results suggested the fluorescence of PDI-nm/*ns*-Q[10]-spermine complex was stable. Consequently, PDI-nm/*ns*-Q[10] has great potential to detect spermine as a highly sensitive fluorescent probe.

In the process of detecting spermine by PDI-nm/*ns*-Q[10] assembly, the thermal stability, pH tolerance and specific selectivity of the assembly were investigated. As various biologically related species exist, including some amino acids (L-tryptophan (L-Trp), L-methionine (L-Met), L-threonine (L-Thr), L-valine (L-Val), L-lysine (L-Lys), L-leucine (L-Leu), L-isoleucine (L-Iso), L-phenylalanine (L-Phe), tyramine (TY), trimethylamine (TMA), dopamine (DA),

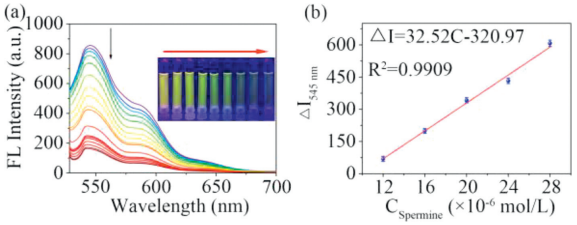

Fig. 4. (a, b) Emission spectra and linear curve of PDI-nm/*ns*-Q[10] toward spermine in the concentration range of 12×10^{-6} – 28×10^{-4} mol/L. Inset: the corresponding photographs under UV-light irradiation at 365 nm.

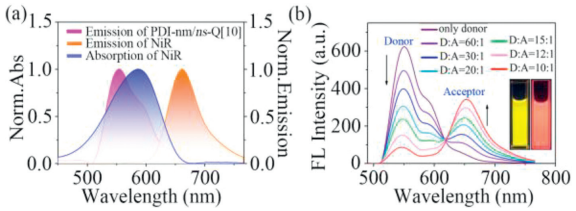

Fig. 5. (a) Normalized emission spectra of PDI-nm/*ns*-Q[10], and absorption and emission spectra of NiR. (b) Fluorescence spectra of PDI-nm/*ns*-Q[10] (PDI-nm/*ns*-Q[10] = 1×10^{-5} mol/L) with different concentration of NiR. The concentrations of NiR was 1×10^{-6} mol/L. Inset: photographs of PDI-nm/*ns*-Q[10], and PDI-nm/*ns*-Q[10]/NiR under UV light (365 nm).

4×10^{-5} mol/L, respectively) and cation/anion (Cu^{2+}, Mn^{2+}, Fe^{3+}, CO_3^{2-}, Br^-, SO_3^{2-}, NO_3^-, HPO_4^{2-}, F^-, 4×10^{-5} mol/L, respectively), under the excitation of 500 nm, the fluorescence change of PDI-nm/*ns*-Q[10] was measured. PDI-nm/*ns*-Q[10] had negligible response to these amino acids and anions/cations (Fig. 3c). Conversely, when PDI-nm/*ns*-Q[10] was mixed with spermine, it showed obvious fluorescence quenching. The influence of temperature on fluorescence was investigated. To imitate the environmental temperature, the temperature values of 10 °C, 20 °C, 30 °C, 40 °C and 50 °C were selected, and the assembly itself showed good temperature stability, and the mixed solution of the assembly with spermine was almost unaffected by temperature (Fig. 3d). Besides, when the pH values were 2, 3, 4, 5, 6, 7, 8, 9 and 10, the fluorescence test showed that the assembly showed excellent pH stability (Fig. S16 in Supporting information).

The satisfactory LOD and high selectivity of PDI-nm/*ns*-Q[10] for spermine, proved that the performance of the fluorescence sensor can be further investigated in real samples. As shown in Fig. 4a, the maximum emission wavelength of PDI-nm/*ns*-Q[10] assembly shifted from 554 nm to 545 nm, it showed that some components in plasma can change the maximum fluorescence emission wavelength of PDI-nm/*ns*-Q[10] assembly. Besides, with the increase of spermine concentration, the fluorescence image of PDI-nm/*ns*-Q[10] assembly can be clearly observed by naked eyes from bright yellow to quenched color. The ratio of emission intensity at 545 nm exhibited a good linear relationship in the with spermine concentration range of 12×10^{-6} mol/L to 28×10^{-4} mol/L (Fig. 4b), which conformed to the following equation: $\Delta I = 32.52C\text{-}320.97$, $R^2 = 0.9909$. And LOD in serum was 3.69×10^{-7} mol/L based on $LOD = 3\sigma/k$. Table S1 (Supporting information) showed the recovery rates for human plasma ranged from 96.54% and 101.93%. The above results indicated that the fast responses and excellent linear relationship provided a real-time quantitative detection method for spermine in biological samples.

The excellent photoluminescence performance and orderly, compact spatial organization of the PDI-nm/*ns*-Q[10] assembly were conducived to its potential application prospect in the preparation of high energy transfer efficiency artificial light-harvesting systems. Subsequently, the hydrophobic fluorescent dye NiR, serving as the energy acceptor, was loaded into the hydrophobic environment of the PDI-nm/*ns*-Q[10] assembly to avoid self-quenching and shorten the distance with donor chromophores, thereby achieving an effective Föster resonance energy transfer (FRET) process. The emission of PDI-nm/*ns*-Q[10] overlaps well with the absorption of NiR (Fig. 5a), promising the feasibility of energy transfer. As depicted in Fig. 5b, a gradual addition of NiR to the PDI-nm/*ns*-Q[10] assembly resulted in a decrease in the fluorescence intensity of the PDI-nm/*ns*-Q[10] assembly (donor) at 554 nm, while the fluorescence emission of NiR (acceptor) at 653 nm increased when excited at 500 nm, indicating an obvious antenna effect at a donor/acceptor ratio of up to 10:1. These results suggested successful loading of NiR into the interior of the PDI-nm/*ns*-Q[10] assembly, with efficient energy transfer from the donor PDI-nm/*ns*-Q[10] to the acceptor NiR in aqueous solution, despite their low concentrations (PDI-nm/*ns*-Q[10] = 1×10^{-5} mol/L and NiR = 1×10^{-6} mol/L), resulting an efficient light-harvesting system in aqueous. The energy transfer efficiency and antenna effect were calculated. Consequently, the energy transfer efficiency was determined to be 87% (Fig. S17 in Supporting information), and the antenna effect was calculated as 6.9 (Fig. S18 in Supporting information) at a donor/acceptor ratio of 10:1. These parameters were crucial for evaluating the light-harvesting ability of an artificial system [44].

In summary, the supramolecular assembly PDI-nm/*ns*-Q[10] acts as a fluorescence indicator displacement assay for the biomolecule spermine. The PDI-nm/*ns*-Q[10] assembly has great application potential in detecting spermine in aqueous solution and in plasma solution. Additionally, in the constructed artificial light-harvesting system experiment, the hydrophobic fluorescent dye NiR was successfully incorporated into the PDI-nm/*ns*-Q[10] supramolecular assembly. This led to a highly efficient energy transfer process from PDI-nm/*ns*-Q[10] to NiR, achieving an energy transfer efficiency of up to 87%. These findings were important for understanding and simulating natural light-harvesting antenna systems. The unique structures and versatile properties of the *ns*-Q[10]-based supramolecular assembly suggested promising future applications in various fields.

Declaration of competing interest

The authors declare that they have no known competing financial interests or personal relationships that could have appeared to influence the work reported in this paper.

Acknowledgment

We acknowledge the support of the National Natural Science Foundation of China (No. 22361011).

Supplementary materials

Supplementary material associated with this article can be found, in the online version, at doi:10.1016/j.cclet.2024.109744.

References

[1] J.L. Rambla, F. Vera-Sirera, M.A. Blazquez, J. Carbonell, A. Granell, Anal. Biochem. 397 (2010) 208–211.
[2] K. Gracie, W.E. Smith, P. Yip, et al., Analyst 139 (2014) 3735–3743.
[3] L. Gerbaut, Clin. Chem. 37 (1991) 2117–2120.
[4] H.P. Til, H.E. Falke, M.K. Prinsen, M.I. Willems, Food Chem. Toxicol. 35 (1997) 337.
[5] G. Gattuso, A. Notti, M.F. Parisi, et al., New J. Chem. 39 (2015) 817–821.
[6] J. Kumpf, J. Freudenberg, S.T. Schwaebel, U.H.F. Bunz, Macromolecules 47 (2014) 2569–2573.
[7] A.C. Sedgwick, J.T. Brewster, T.H. Wu, et al., Chem. Soc. Rev. 50 (2021) 9–38.
[8] J.S. Wu, B. Kwon, W.M. Liu, et al., Chem. Rev. 115 (2015) 7893–7943.
[9] B.T. Nguyen, E.V. Anslyn, Coord. Chem. Rev. 250 (2006) 3118–3127.

[10] I.A. Rather, R. Ali, Org. Biomol. Chem. 19 (2021) 5926–5981.
[11] H.Q. Peng, L.Y. Niu, Y.Z. Chen, et al., Chem. Rev. 115 (2015) 7502–7542.
[12] S. Saha, J.F. Stoddart, Chem. Soc. Rev. 36 (2007) 77–92.
[13] Z. Zhang, Z. Zhao, Y. Hou, et al., Angew. Chem. Int. Ed. 58 (2019) 8862–8866.
[14] J. Yang, M.C. Yoon, H. Yoo, P. Kim, D. Kim, Chem. Soc. Rev. 41 (2012) 4808–4826.
[15] H.Q. Peng, Y.Z. Chen, Y. Zhao, et al., Angew. Chem. Int. Ed. 51 (2012) 2088–2092.
[16] L.B. Meng, D. Li, S. Xiong, et al., Chem. Commun. 51 (2015) 4643–4646.
[17] Z. Xu, S. Peng, Y.Y. Wang, et al., Adv. Mater. 28 (2016) 7666–7671.
[18] D. Yang, M. Liu, X. Xiao, Z. Tao, C. Redshaw, Coordination Chem. Rev. 434 (2021) 213733.
[19] R. Cen, M. Liu, J. He, et al., Chin. Chem. Lett. 34 (2023) 108195.
[20] M. Liu, R. Cen, J. Zhao, et al., Separ. Purif. Technol. 304 (2023) 122342.
[21] Y. Luo, W. Zhang, J. Zhao, et al., Chin. Chem. Lett. 34 (2023) 107780.
[22] M. Liu, L.X. Chen, P.H. Shan, et al., ACS Appl. Mater. Interfaces 13 (2021) 7434–7442.
[23] J. Wu, L. Isaacs, Chem. Eur. J. 15 (2009) 11675–11680.
[24] M. Florea, W.M. Nau, Angew. Chem. Int. Ed. 50 (2011) 9338–9342.
[25] W.H. Huang, S.M. Liu, P.Y. Zavalij, L. Isaacs, J. Am. Chem. Soc. 128 (2006) 14744–14745.
[26] D. Lucas, T. Minami, G. Iannuzzi, et al., J. Am. Chem. Soc. 133 (2011) 17966–17976.
[27] L. Isaacs, Acc. Chem. Res. 47 (2014) 2052–2062.
[28] R. Cen, M. Liu, H. Xiao, et al., Sens. Actuat. B: Chem. 378 (2023) 133126.
[29] M. Liu, R. Cen, J.S. Li, et al., Angew. Chem. Int. Ed. 61 (2022) e202207209.
[30] X.D. Zhang, W. Wu, Z. Tao, X.L. Ni, Beilstein J. Org. Chem. 15 (2019) 1705–1711.
[31] K.M. Park, J.H. Roh, G. Sung, J. Murray, K. Kim, Chem. Asian J. 12 (2017) 1461–1464.
[32] E.A. Appel, J.D. Barrio, J. Dyson, L. Isaacsb, O.A. Scherman, Chem. Sci. 3 (2012) 2278–2281.
[33] G. Carroy, V. Lemaur, J.D. Winter, et al., Phys. Chem. Chem. Phys. 18 (2016) 12557–12568.
[34] Y.C. Yang, X.L. Ni, J.F. Xu, X. Zhang, Chem. Commun. 55 (2019) 13836–13839.
[35] P.Q. Zhang, Q. Li, Z.K. Wang, et al., Chin. Chem. Lett. 34 (2022) 107632.
[36] Z. Chen, A. Lohr, C.R. Saha-Moller, F. Wurthner, Chem. Soc. Rev. 38 (2009) 564–584.
[37] F. Wurthner, Chem. Commun. 14 (2004) 1564–1579.
[38] F. Biedermann, E. Elmalem, I. Ghosh, W.M. Nau, O.A. Scherman, Angew. Chem. Int. Ed. 51 (2012) 7739–7743.
[39] C. Wang, Z.Q. Wang, X. Zhang, Acc. Chem. Res. 45 (2012) 608–618.
[40] D.S. Guo, K. Wang, Y.X. Wang, Y. Liu, J. Am. Chem. Soc. 134 (2012) 10244–10250.
[41] W.L. Mock, N.Y. Shih, Structure and selectivity in host-guest complexes of cucurbituril, J. Org. Chem. 51 (1986) 4440–4446.
[42] C.D.P.C. Carvalho, Supramolecular biomimetic binding of the DNA-dye hoechst 33258 by a synthetic macrocycle, The University of the Algarve, 2010 Master Dissertation.
[43] Y. Liu, Y. Yu, J. Gao, Z. Wang, X. Zhang, Angew. Chem. Int. Ed. 49 (2010) 6576–6579.
[44] Z. Xu, S. Peng, Y.Y. Wang, et al., Adv. Mater. 28 (2016) 7666.